Synthesis and Characterization of Hyperbranched Polymers with Increased Chemical Versatility for Imprint Lithographic Resists

ANZAR KHAN,[1] MICHAEL MALKOCH,[1,2] MARTHA F. MONTAGUE,[3,4] CRAIG J. HAWKER[1]

[1]Materials Research Laboratory, Department of Chemistry and Materials, University of California, Santa Barbara, California 93106

[2]Fiber and Polymer Technology, Royal Institute of Technology, Teknikringen 56-58, SE-10044 Stockholm, Sweden

[3]Center for Nanotechnology and Department of Chemical and Biological Engineering, University of Wisconsin, Madison, Wisconsin 53706

[4]IBM Almaden Research Center, San Jose, California 95120

Received 16 May 2008; accepted 10 June 2008
DOI: 10.1002/pola.22934
Published online in Wiley InterScience (www.interscience.wiley.com).

ABSTRACT: Hyperbranched polymers were prepared from a variety of mono- and difunctional monomers and used in the development of novel UV-imprint lithography (UV-IL) resists. The unique physical and chemical properties of these hyperbranched materials significantly increase the range of molecular systems that could be imprinted. Traditional challenges, such as the use of monomers that have low boiling points or the use of insoluble/highly crystalline momomers, are overcome by the preparation of hyperbranched polymers that incorporate these repeat units. In addition, the low viscosity of the hyperbranched macromolecules and the large number of reactive chain ends overcome many difficulties that are traditionally associated with the use of polymeric materials as imprint resists. Hyperbranched polymers containing up to 12 mol % pendant vinyl groups, needed for secondary crosslinking during imprinting, were prepared with a wide range of repeat unit structures and successfully imprinted with features from tens of microns to $\sim$ 100 nm. © 2008 Wiley Periodicals, Inc. J Polym Sci Part A: Polym Chem 46: 6238–6254, 2008
Keywords: hyperbranched; imprint lithography; living radical polymerization; photopolymerization; resists

INTRODUCTION

Imprint lithography, in which a stamp is pressed into an organic film resulting in pattern transfer, has not only demonstrated nanoscale resolution but is also a simple and relatively inexpensive technique for the fabrication of many nanoscale structures.[1–3] As a result, imprint lithography finds application in a range of industries, in particular in microelectronics where critical dimensions are shrinking below 50 nm, whereas traditional optical lithography is becoming increasingly complex and expensive.[4] A number of variations on imprint lithography have been developed, including those that use solvent[5,6] or

Correspondence to: C. J. Hawker (E-mail: hawker@mrl.ucsb.edu)

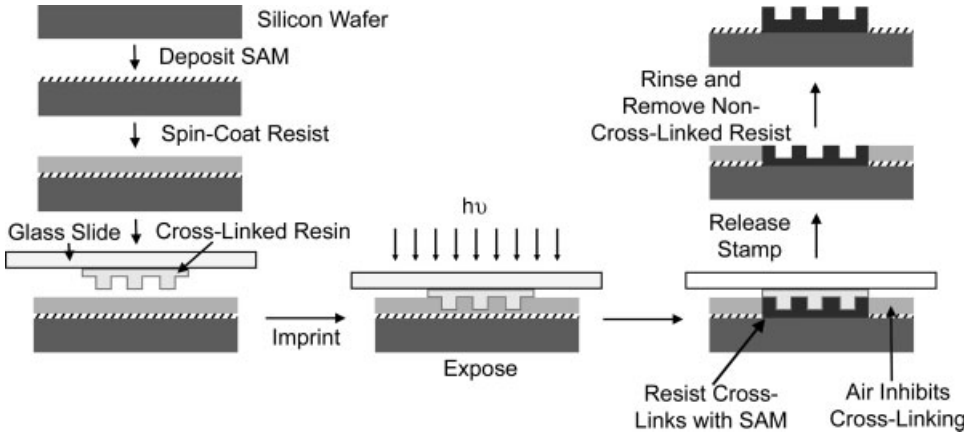

Figure 1. Process scheme for patterning with UV-IL system developed by McClelland et al.[12]

heat[7,8] during imprinting to improve the flow of the resist, the most promising technique is based on UV curing (UV-imprint lithography or UV-IL) (Fig. 1).[9–12] In these systems, the stamp is designed to be transparent to UV light, and the resist materials are typically low viscosity, multifunctional monomers that crosslink upon exposure. The stamp is irradiated during imprinting, which crosslinks the resist and allows for the stamp to be removed while still retaining the pattern.

Although the principles of UV-IL are simple, for this technique to be used for the manufacture of integrated circuits or other devices, there are a number of engineering problems that must be addressed. Processing conditions need to be optimized for the best resist flow to completely fill the features while exposure times should be minimized by using appropriate polymerization chemistries in the resist.[13] In the stamp release step, adhesion of the resist needs to be reduced, which can be accomplished by varying the surface chemistry of the stamp.[14–16] In the printing of multilevel devices, accurate alignment of the stamp during each imprint is crucial,[17] the solubility of the crosslinked imprint material should be enhanced for efficient cleaning of templates,[18] and an understanding and minimization of defect generation is also required.[19]

Although these issues are important to traditional applications of UV-IL, possibly the most significant issue for wide-scale adoption is the ability to incorporate different chemistries into the resist.[20–22] For standard microelectronics applications, resists should be designed to maximize resistance to the various etches needed for pattern transfer. However, to increase the impact of UV-IL, the resists must be tailored to a broad range of applications, including biocompatible substrates[23,24] or nano-fluidics,[25,26] and therefore the resist system should be compatible with a variety of chemistries. To incorporate different chemistries into the UV-IL resists, there are a number of limitations that are imposed by the processing requirements of this system. The resist films are usually applied by spin-coating the desired mixture of monomers onto the substrate. Therefore, the UV-curable monomers need to be soluble in good solvents for spin-coating. Additionally, the monomers must not evaporate during spin-coating and therefore should possess a high boiling point. Finally, dewetting of the resist solution during the length of time necessary to spin-coat and imprint the film leads to an unusable material. As a result, the combination of all of these requirements for resist materials dramatically restricts

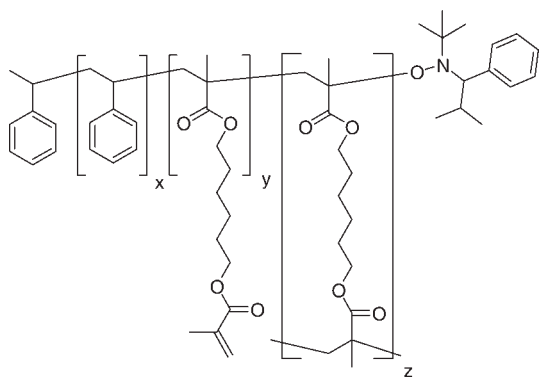

Figure 2. Structure of hyperbranched polymer, **1**, prepared from styrene and 1,6-hexanediol dimethacrylate.

the monomers that can be used in traditional UV-based imprint patterning system.

One potential method for avoiding these problems is the use of low molecular weight, highly branched polymers,[27,28] with advantages that include reduced dewetting, no evaporation, low viscosity, and a large number of reactive chain ends. Additionally, formation of a polymer from a low solubility or crystalline monomer significantly increases the solubility of the corresponding repeat unit in spin-coating solvents. In developing a method for preparing hyperbranched polymers for UV-IL, the important characteristics are branching (to obtain low viscosity resist solutions), ability to control the chemical composition of the hyperbranched polymer, compatibility with a wide range of monomers, and a simple, high yielding synthesis.

Previously, hyperbranched polymers have been synthesized from condensation of AB_x monomers,[29] inimers by self-condensing vinyl polymerizations,[30] and from mixtures of monofunctional and difunctional (crosslinking) monomers, using traditional free radical polymerization techniques[31,32] as well as nitroxide-mediated radical polymerization (NMRP) techniques.[33,34] In these cases, the polymers were found to contain singly polymerized crosslinkers containing pendant polymerizable groups, demonstrating the potential of these materials for UV-IL applications. In the preparation of hyperbranched polymers by normal free radical polymerization methods, high amounts of chain transfer agent (CTA), usually a ratio of 1:1 CTA to crosslinker, were needed to prevent gelling.[31] As a significant amount of pendant polymerizable groups are needed in the hyperbranched polymer to ensure a high crosslink density in UV-IL applications, a correspondingly high fraction of crosslinker is therefore needed in the initial monomer solution. For free radical polymerization, this would then require a large amount of CTA resulting in reduced control over the chemical composition of the material. In comparison, NMRP techniques do not require the use of CTA and by controlling the concentrations of crosslinker and initiator, conversion as high as 90% has been reported without gelation.[33,34] A drawback of this method is that it has not been examined for mole fractions of crosslinker greater than 4%, which is too low for UV-IL applications. To overcome these limitations, this manuscript examines the preparation of functional hyperbranched polymers from a variety of monomers for UV-IL applications that have significant flexibility in the choice of repeat units, which subsequently translates into performance versatility by NMRP.

EXPERIMENTAL

Materials

All chemicals were obtained from Aldrich and used without further purification unless otherwise noted. Dichloromethane was distilled under argon over calcium hydride. Methacryloyl chloride and triethylamine were distilled once under argon. THF was distilled under nitrogen over sodium/benzophenone. Analytical thin-layer chromatography was performed on commercial Merck plates coated with silica gel GF254 (0.25-mm thick). Flash chromatography was performed on Merck Kiselgel 60 (230–400 mesh). Silicon wafers (1″, <100>) were obtained from Virginia Semiconductor. 2,5-Dimethyl-2,5-hexanediol dimethacrylate[35] and 2,2,5-trimethyl-3-(1-phenylethoxy)-4-phenyl-3-azahexane[36] were synthesized according to literature procedures.

Materials Characterization

NMR spectra were recorded on Bruker Advance 400 (250.1 and 62.9 MHz for ^{1}H and ^{13}C, respectively), spectrometer at 23 ± 2 °C using the solvent signal as internal standard (^{1}H: $\delta(CHCl_3)$ = 7.24 ppm, δ(DMSO) = 2.49, and ^{13}C: $\delta(CHCl_3)$ = 77.0 ppm, δ(DMSO) = 39.7 ppm). Gas Chromatography was performed on a Hewlett-Packard 5890 Series II with a Spectra-Physics Analytical SP4270 Integrator. GPC measurements were performed on Waters Corporation 515 HPLC pump equipped with 410 Differential Refractometer, 996 Photodiode Array Detector, and high-resolution analytical columns (7.8 × 300 mm) in series (Styragel® HR 5E to HR 4E to HR2 to HR1). The measurements were performed in THF at 30 °C using a flow rate of 1 mL/min. The columns were calibrated with several narrow polydispersity (PDI) polystyrene samples. Molecular weights were also determined by multiangle laser light scattering using a Wyatt Technologies Dawn-EOS photogoniometer in the static mode, at 632 nm and 25 °C. FTIR spectra were obtained of thin films on KBr using a Nicolet Nexus 870 FTIR. Thermogravimetric Analysis (TGA) was performed on a TA Instruments TGA-2950 at a heating rate of 10 °C/min under nitrogen atmosphere. Differential Scanning Calorimetry measurements

were performed on a TA Instruments MDSC Q1000 at a heating rate of 10 °C/min under nitrogen and modulated at ±0.6 °C/min.

Surface Characterization

Atomic force microscopy (AFM) was performed on a Digital Instruments Dimension 3100 with a NanoScope IV controller. Images were obtained with a scan rate of 0.500 Hz for 50-μm scan sizes and 1.000 Hz for 1- and 5-μm scan sizes. Scanning electron microscopy (SEM) was done on a Hitachi *S*-4700, using a current of 1.0 kV. Optical micrographs were obtained with an Olympus Vanox optical microscope and a SPOT RT color digital camera with the associated SPOT Basic software (Diagnostic Instruments). Film thicknesses were measured by both ellipsometry and profilometry. The profilometer was a Tencor Instruments alpha-step 200. Ellipsometric film thicknesses were calculated using the Gaertner Ellipsometer Measurement Program and delta and psi values obtained from a Gaertner Scientific Variable Angle Stokes Ellipsometer L116SF. Ellipsometry measurements were done at an angle of 70° with a wavelength of 632.8 nm. For the calculations, the N_s and K_s values for the silicon substrate were taken as 3.881 and −0.018, respectively. The silicon oxide layer was assumed to be 2.0-nm thick with a refractive index of 1.457, and the refractive index of the organic film was assumed to be 1.5.

Hyperbranched Polymer Preparation (General Procedure)

Styrene (3.90 g, 37.5 mmol), 1,6-hexanediol dimethacrylate (3.175 g, 12.5 mmol), and initiator (2,2,5-trimethyl-3-(1-phenylethoxy)-4-phenyl-3-azahexane) (325 mg, 1 mmol) were mixed and diluted to the desired "solids" concentration in toluene between 8 and 75 wt %. The monomer solution was placed in an ampule with a stir bar, degassed by three freeze/thaw cycles, and sealed under vacuum. The polymerization was carried out at 125 °C for times ranging from 0.5 to 5 h. Hyperbranched polymers were purified by precipitating the toluene solution into methanol. The insolubles were collected using centrifugation and dried to remove any residual solvent. The crude hyperbranched polymer was precipitated a second time by first dissolving into a minimal amount of dichloromethane and then precipitating into methanol. The hyperbranched polymer, **1**, was collected by filtration and dried under vacuum to remove residual solvent; for 15 wt %, yield = 52%, M_n = 7400, PDI = 3.9.

^{1}H NMR (CD_2Cl_2) δ 7.60–6.40 (br m, 24.8H, Ar*H*), 6.09 (br s, 1H, C=CH_2), 5.56 (br s, 1H, C=CH_2), 4.40–2.90 (br m, 8.4H, OCH_2), 2.70–0.50 (br m, 67.3H, $OCH_2CH_2CH_2$, $CH_2C(CH_3)COOR$, CH_2CHAr). IR (neat) 2937, 1719, 1454, 1167, 700 cm^{-1}.

Methyl Methacrylate-Based Hyperbranched Polymer, 2 (Example of Low Boiling Point Monomer)

This was prepared using the general hyperbranched polymer polymerization procedure, that is, from an initial monomer mixture of methyl methacrylate (MMA; 3.75 g, 37.5 mmol), 1,6-hexanediol dimethacrylate (3.175 g, 12.5 mmol), and initiator (325 mg, 1 mmol), which was then diluted to 8 wt % in toluene. The solution was allowed to polymerize for 2 h and the resultant crude hyperbranched polymer was purified by removal of the MMA and toluene under reduced pressure to obtain a 62% yield. The crude hyperbranched polymer could be further purified by precipitation from THF into cold methanol to give **2** as a white solid. M_n = 7300, PDI = 2.4.

^{1}H NMR ($CDCl_3$) δ 6.10 (br s, 2.0H, CH_2=C), 5.56 (br s, 2.0H, CH_2=C), 4.30–3.40 (br m, 4.7H, OCH_2, OCH_3), 2.30–0.60 (br m, 16.1H, OCH_2CH_2 CH_2, $CH_2C(CH_3)COOR$). IR (neat) 2951, 1724, 1720, 1716, 1166 cm^{-1}.

Dimethacrylate Diacetal Benzene-Based Hyperbranched Polymer, 3 (Example of Low Solubility Monomer)

This was prepared using the general hyperbranched polymer polymerization procedure, that is, from an initial monomer mixture of *p*-acetoxy styrene (6.075 g, 37.5 mmol), dimethacrylate diacetal benzene (DMDAB; 3.175 g, 12.5 mmol), and initiator (325 mg, 1 mmol), which was then diluted to 8 wt % in 1:1 toluene:dioxane. The solution was allowed to polymerize for 2 h, and the resultant crude hyperbranched polymer was concentrated by removal of the toluene and dioxane under reduced pressure. The crude hyperbranched polymer was redissolved in THF, filtered through a 0.2 μm PTFE filter, and concentrated under reduced pressure. The crude hyperbranched polymer could be further purified by precipitation from THF into cold methanol to remove the excess *p*-acetoxy styrene to give **3**, yield = 48%, M_n = 9000, PDI = 2.3.

^{1}H NMR ($CDCl_3$) δ 7.53 (s, 4.2H, Ar*H* from DMDAB), 7.42 (d, J = 8.4 Hz, 8.8H, CH_2=CHAr*H*), 7.06 (d, J = 8.4 Hz, 8.8H, CH_2=CHAr*H*), 6.71 (dd, J = 10.8, 18.0 Hz, 4.4H, CH_2=C*H*), 6.29 (s, 1.1H, CH_2=, dioxanyl), 6.13 (s, 1.0H, CH_2=, dioxolanyl), 5.71 (d, J = 17.2 Hz, 4.4H, CH_2=CH), 5.65 (s, 1.1H, CH_2=, dioxanyl), 5.63 (s, 1.0H, CH_2=, dioxolanyl), 5.58 (s, 1.1H, C*H*Ar, dioxanyl), 5.49 (s, 1.0H, C*H*Ar, dioxolanyl), 5.25 (d, J = 10.4 Hz, 4.4H, CH_2=CH), 5.13–5.02 (m, 1.0H, C*H*CH$_2$OC=O, dioxolanyl), 4.77 (s, 1.1H, C*H*OC=O, dioxanyl), 4.43 (dd, J = 5.2 and 10.0 Hz, 2.0H, CH_2OC=O, dioxolanyl), 4.26 (dd, J = 13.0 and 52.6 Hz, 4.4H, CHCH_2O, dioxanyl), 3.81–3.70 (m, 2.0H, OCH_2CH, dioxolanyl), 2.31 (s, 13.2H, (CH_3)COOAr), 2.00 (s, 3.3H, CH_3, dioxanyl), 1.95 (s, 3.0H, CH_3, dioxolanyl). IR (neat) 2982, 2929, 2863, 1762, 1720, 1506, 1369, 195, 1166, 1144, 1104, 1084, 1014, 911 cm^{-1}.

Silyl-Based Hyperbranched Polymer, 4 (Example of Dewetting Monomer)

This was prepared using the general hyperbranched polymer polymerization procedure, from an initial monomer mixture of 3-acryoyloxypropyl tris(trimethylsiloxy)silane, APTMS (15.3 g, 37.5 mmol), 1,6-hexanediol dimethacrylate (3.175 g, 12.5 mmol), and initiator (325 mg, 1 mmol), which was then diluted to 8 wt % in toluene. The solution was allowed to polymerize for 2 h and then concentrated by removal of the toluene under reduced pressure. The crude hyperbranched polymer was redissolved into THF and precipitated into cold methanol to obtain a 29% yield of the silyl substituted hyperbranched polymer, **4**. M_n = 14,900, PDI = 2.9.

^{1}H NMR ($CDCl_3$) δ 6.10 (br s, 1H, C=CH_2), 5.55 (br s, 1H, C=CH_2), 4.50–3.27 (br m, 28H, OCH_2), 2.76–0.00 (br m, 300H, CH_2C(CH_3)COOR, SiCH_2CH_2, Si(CH_3)$_3$). IR (neat) 2957, 1732, 1252, 1150, 1056, 843, 756 cm^{-1}.

DHDMA-Based Hyperbranched Polymer, 5 (Example of Incorporating an Acid-Cleavable Monomer)

This was prepared using the general hyperbranched polymer polymerization procedure, that is, from an initial monomer mixture of *p*-acetoxy styrene (6.075 g, 37.5 mmol), 2,5-dimethyl-2,5-hexanediol dimethacrylate (3.30 g, 12.5 mmol), and initiator (325 mg, 1 mmol), which was then diluted to 8 wt % in toluene. The solution was allowed to polymerize for 2 h and the resultant crude hyperbranched polymer was concentrated by removal of the toluene under reduced pressure. The crude hyperbranched polymer could be further purified by precipitation into cold hexane to the pure product, **5**, as a white solid (64%). M_n = 1800, PDI = 1.2.

^{1}H NMR (CD_2Cl_2) δ 7.42 (d, J = 8.4 Hz , 6.6H, Ar*H*), 7.06 (d, J = 8.4 Hz, 6.6H, Ar*H*), 6.71 (dd, J = 11.0, 17.8 Hz, 3.3H CH$_2$=C*H*Ar), 6.02 (s, 2.0H, CH_2=C(CH$_3$)), 5.71 (d, J = 18.4 Hz, 3.3H, CH_2=CHAr), 5.50 (s, 2.0H, CH_2=C(CH$_3$)), 5.25 (d, J = 11.6 Hz, 3.3H, CH_2=CHAr), 2.31 (s, 9.9H, CH_3COO), 1.91 (s, 6.0H, CH_2CH_2), 1.85 (s, 4.0H, =CCH_3), 1.49 (s, 12.0H, C(CH_3)$_2$). IR (neat) 2979, 1767, 1712, 1506, 1207, 1194 cm^{-1}.

General Hyperbranched Polymer Imprinting Procedure

The stamp fabrication, substrate preparation, and imprinting procedures used were described by von Werne et al.[20] and McClelland et al.[12] The hyperbranched polymer resin solution was initially mixed with 2 wt % 2,2-dimethoxy-2-phenylacetophenone and then diluted in an appropriate solvent for spin-coating at the desired concentration. The solution (0.2 mL) was filtered through a 0.45-μm PTFE filter onto a wafer coated with a self-assembled monolayer of adhesion promoter (3-methacryoxypropyl trimethoxysilane) and spin-coated at 3000 rpm for 30 s. The stamp was placed on top of the coated wafer followed by a flat disc of PDMS on top of the stamp, and then an Instron 5500R and the associated Merlin software were used to apply a force which was ramped up to 400N. After the necessary hold time has passed, the sample was exposed to 20 J/cm^2 of 365 nm radiation (OAI Model 30 light source, 33 mW). The applied force was then removed from the sample, and the stamp was removed from the wafer using either heat or a 1% Liquinox water solution to improve stamp release. The wafer was then rinsed with acetone and isopropanol while spinning on a spin-coater to remove the unreacted resin, leaving behind the crosslinked film attached to the silicon wafer.

Specific Hyperbranched Polymer Imprint Conditions

Hyperbranched Polymer from a Low Boiling Point Monomer

The resin consisted of the crude hyperbranched polymer without further dilution, and the spin-

coating solvent was propylene glycol methyl ether acetate (PGMEA). The hold time was 5 min and the stamp release method was heat.

Hyperbranched Polymer from a Low Solubility Soluble Monomer

The resin consisted of the crude hyperbranched polymer diluted to 25 wt % in *p*-acetoxy styrene, and the spin-coating solvent was chlorobenzene. The hold time was 30 min and the stamp release method was Liquinox.

Hyperbranched Polymer from a Dewetting Monomer

The resin consisted of the precipitated hyperbranched polymer diluted to 50 wt % in 1,6-hexanediol dimethacrylate, and the spin-coating solvent was PGMEA. The hold time was 5 min and the stamp release method was heat.

Hyperbranched Polymer Incorporating a Functional Crosslinker

The resin consisted of the crude hyperbranched polymer without further dilution, and the spin-coating solvent was PGMEA. The hold time was 5 min and the stamp release method was Liquinox.

Lithographic Patterning of DHDMA and DMDAB Hyperbranched Polymer Cross-Linked Films

A solution of polystyrene (6000 g/mol, 10%) and PAG (bis(*tert*-butyl phenyl) iodonium triflate (1%) in PGMEA was spin-coated at 2500 rpm for 60 s to create a 200 nm thick layer. TEM grids (TED Pella, nickel, 1000 mesh) were then placed on top of the PAG/PS film while the samples were exposed to 254-nm radiation (OAI Model 30 light source and a 254 nm filter, 0.74 mW). After removing the TEM grids, the samples were baked on a hot plate and rinsed with toluene and acetone, alternating two times with each, to remove the polymer layer and any decomposed film, before drying under a stream of nitrogen. The sample was placed in a 28% solution of ammonium hydroxide for 5 min, rinsed with water and ethanol, and dried under a stream of nitrogen.

Determination of Etch Rate

Films were etched using an Inductively Coupled Plasma etch tool from Surface Technology Systems, which operated with an oxygen flow rate of 30 sccm, a pressure of 6 mTorr, a coil power of 300 W, a platen power of 20 W, and a platen temperature of 20 °C. The resultant DC and AC biases with silicon wafers were 110 and 350 V, respectively. To determine the etch rate, capillary tubes were placed on top of the wafers, and the height change was measured with both ellipsometry and profilometry.

DMDAB Synthesis: (i) Diol Diacetal Benzene, 6

A solution of glycerol (5.00 g, 54.3 mmol), terephthaldicarboxaldehyde (3.46 g, 25.9 mmol), and *p*-toluenesulfonic acid (0.25 g, 1.3 mmol) in benzene (500 mL) was heated to reflux using a Dean-Stark trap for 14 h until $\sim$ 0.90 mL (50 mmol) of water was collected. The PTSA was neutralized with an excess of a 1:1 solution of ethanol and ammonium hydroxide (28%), dissolved in a minimal amount of THF, and filtered to remove the PTSA salts. The THF solution was precipitated into water (500 mL). The solids were filtered, dried, redissolved in THF, and then precipitated in ether. The precipitate was filtered and dried to obtain the product, **6**, as a white powder (6.50 g, 90%), a mixture of three structural isomers: benzene 1,4-di(5-hydroxy-[1,3]dioxanyl), benzene 1,4-di (4-hydroxymethyl-[1,3]dioxolanyl), and benzene 1-(5-hydroxy-[1,3]dioxanyl)-4-(4-hydroxymethyl-[1,3]dioxolanyl). The ratio of dioxanyl to dioxolanyl groups was 1:1.2.

^{1}H NMR (DMSO-d_6) δ 7.46–7.37 (m, 4H, Ar*H*), 5.54 (s, 1H, C*H*Ar, dioxanyl), 5.42 (s, 1H, C*H*Ar, dioxolanyl), 4.16–4.10 (m, 2H, CH_2OH, dioxolanyl), 3.99 (dd, J = 12.0 and 40.2 Hz, 4H, CH_2CHOH, dioxanyl), 3.76–3.66 (m, 1H, C*H*CH$_2$OH, dioxolanyl), 3.48 (dd, J = 10.4 and 10.4 Hz, 2H, OCH_2CH, dioxolanyl), 3.50 (s, 1H, (CH$_2$)$_2$C*H*O, dioxanyl). ^{13}C NMR (DMSO-d_6) δ 139.48, 139.09, 138.47, 138.37, 125.92, 125.86, 125.84, 125.72, 99.99, 99.97, 99.92, 71.64, 71.40, 63.10, 62.39, 60.23. IR (neat) 3347, 2868, 1386, 1095, 991, 784 cm^{-1}.

DMDAB Synthesis: (ii) Mixture of Three Structural Isomers, 7, 8, and 9

Methacrylic anhydride (35.7 mmol, 5.86 g), **6** (7.14 mmol, 2.00 g), 4-dimethylaminopyridine (2.1 mmol, 0.80 g), and anhydrous triethylamine (71.4 mmol, 7.20 g) were dissolved in a mixture of anhydrous THF (300 mL) and anhydrous dichloromethane (50 mL) and stirred at room temperature

for 14 h. The solvents were evaporated, and the solids were dissolved in a minimal amount of dichloromethane and precipitated in hexane (500 mL). The precipitate was filtered, dried, and purified by column chromatography, eluting with 1:1 hexane:ethyl acetate, shifting to ethyl acetate and then 9:1 ethyl acetate:dichloromethane to isolate the mixture of three structural isomers as white powders (1.66 g, 52%).

^{1}H NMR ($CDCl_3$) δ 7.51 (s, 4H, Ar*H*), 6.27 (s, 1H, CH_2=, dioxanyl), 6.12 (s, 1H, CH_2=, dioxolanyl), 5.64 (s, 1H, CH_2=, dioxanyl), 5.62 (s, 1H, CH_2=, dioxolanyl), 5.57 (s, 1H, C*H*Ar, dioxanyl), 5.48 (s, 1H, C*H*Ar, dioxolanyl), 5.10–5.03 (m, 1H, C*H*CH$_2$OC=O, dioxolanyl), 4.75 (s, 1H, C*H*OC=O, dioxanyl), 4.42 (dd, J = 5.2 and 11.2 Hz, 2H, CH_2OC=O, dioxolanyl), 4.24 (dd, J = 12.8 and 52.8 Hz, 4H, CHCH_2O, dioxanyl), 3.74 (dd, J = 10.0 and 11.2 Hz, 2H, OCH_2CH, dioxolanyl), 2.00 (s, 3H, CH_3, dioxanyl), 1.94 (s, 3H, CH_3, dioxolanyl). ^{13}C NMR δ 167.41, 166.36, 138.97, 138.27, 136.26, 135.89, 126.79, 126.69, 126.39, 126.37, 126.31, 126.27, 101.18, 101.11, 101.10, 69.18, 68.70, 68.68, 66.33, 63.13, 63.11, 18.47, 18.45. IR (neat) 2986, 2963, 2867, 1718, 1163, 1143, 1104, 1085, 1013, 988 cm^{-1}.

The three structural isomers could be separated from the mixture by flash chromatography, eluting with hexane, increasing to 1:1 hexane:ethyl acetate, then ethyl acetate, and finally 9:1 ethyl acetate:dichloromethane.

1,4-Di(5-methacryloyloxy-[1,3]dioxanyl) Benzene, 7

^{1}H NMR ($CDCl_3$) δ 7.52 (s, 4H, Ar*H*), 6.27 (s, 2H, CH_2=), 5.63 (s, 2H, CH_2=), 5.57 (s, 2H, C*H*ArHC*H*), 4.75 (s, 2H, C*H*OC=O), 4.24 (dd, J = 12.4 and 52.4 Hz, 8H, CHCH_2O), 2.00 (s, 6H, CH_3). ^{13}C NMR δ 167.37, 138.96, 136.24, 126.74, 126.25, 101.08, 69.15, 66.32, 18.42. Melting point = 206 °C.

1-(5-Methacryloyloxy-[1,3]dioxanyl)-4-(4-methacryloyloxymethyl-[1,3]dioxolanyl) Benzene, 8

^{1}H NMR ($CDCl_3$) δ 7.51 (s, 4H, Ar*H*), 6.27 (s, 1H, CH_2=, dioxanyl), 6.12 (s, 1H, CH_2=, dioxolanyl), 5.64 (s, 1H, CH_2=, dioxanyl), 5.62 (s, 1H, CH_2=, dioxolanyl), 5.57 (s, 1H, C*H*Ar, dioxanyl), 5.48 (s, 1H, C*H*Ar, dioxolanyl), 5.10–5.03 (m, 1H, C*H*CH$_2$OC=O, dioxolanyl), 4.75 (s, 1H, C*H*OC=O, dioxanyl), 4.42 (dd, J = 5.2 and 11.2 Hz, 2H, CH_2OC=O, dioxolanyl), 4.24 (dd, J = 12.8 and 52.8 Hz, 4H, CHCH_2O, dioxanyl), 3.74 (dd, J = 10.0 and 11.2 Hz, 2H, OCH_2CH, dioxolanyl), 2.00 (s, 3H, CH_3, dioxanyl), 1.94 (s, 3H, CH_3, dioxolanyl). ^{13}C NMR δ 167.34, 166.30, 138.95, 138.22, 136.20, 135.83, 126.72, 126.64, 126.31, 126.25, 101.13, 101.03, 69.13, 68.62, 66.29, 63.09, 18.41, 18.39. Melting point = 191 °C.

1,4-Di(4-methacryloyloxymethyl-[1,3]dioxolanyl) Benzene, 9

^{1}H NMR ($CDCl_3$) δ 7.51 (s, 4H, Ar*H*), 6.12 (s, 2H, CH_2=), 5.62 (s, 2H, CH_2=), 5.48 (s, 2H, C*H*ArHC*H*), 5.11–5.04 (m, 2H, C*H*CH$_2$OC=O), 4.42 (dd, J = 5.2 and 11.2 Hz, 4H, CH_2OC=O), 3.74 (dd, J = 10.0 and 11.2 Hz, 4H, OCH_2CH), 1.94 (s, 6H, CH_3). ^{13}C NMR δ 166.36, 138.29, 135.90, 126.69, 126.40, 101.18, 68.71, 63.12, 18.47. Melting point = 228 °C.

RESULTS AND DISCUSSION

Hyperbranched Polymer Synthesis and Characterization

The formation of high-resolution images with UV-IL is highly dependant on the physical and chemical properties of the resist, in particular on the ability of the material both to flow into the features and subsequently form highly crosslinked networks with dimensional stability.[9] These processing characteristics are directly related to the structure of the material, in particular viscosity and availability of functional groups. While linear polymers suffer from entanglement dominated viscosity profiles and only a limited number of chain end functional groups, hyperbranched polymers have been shown to have very low melt and solution viscosities, resembling dendritic macromolecules, as well as an abundance of reactive chain end groups. As a result, hyperbranched macromolecules have a number of intrinsic advantages when compared with linear polymers and monomer mixtures for use in imprint lithography. The synthesis of hyperbranched macromolecules by the controlled copolymerization of vinyl monomers with divinyl crosslinking materials was therefore examined and techniques for controlling the hyperbranched polymer structure and composition by varying the polymerization conditions elucidated. The variables that were studied included polymerization time, molar ratio of monomers to initiator, and concentration of the polymerization mixture. NMRP using 2,2,5-

trimethyl-3-(1-phenylethoxy)-4-phenyl-3-azahexane[36] as the initiator was examined with toluene as the solvent to allow for comparison with corresponding traditional free radical studies.[29–32,37] For all experiments, a 3:1 ratio of monofunctional monomer to crosslinker was used. Although this concentration of crosslinker is significantly higher than that used in other reports, namely 12% for free radical polymerizations[31] and 4% for NMRP,[34] it was due to the desire to have a high concentration of pendant vinyl groups in the hyperbranched polymer, which allows for secondary crosslinking and nanometer scale dimensional stability (Fig. 2).

To understand the evolution of the polymer structure during polymerization, samples were prepared and heated at 125 °C for 30, 60, 90, 120, 150, 180, 210, 240, 270, and 300 min. For these experiments, the monomers used were styrene and 1,6-hexanediol dimethacrylate and the total molar ratio of monomer to initiator was 50:1, chosen to keep molecular weights low, branching high while ensuring that the initiator does not form a large mass fraction of the hyperbranched polymer. The total conversion of monomer was found to increase over time, reaching ~ 50% conversion after 3 h [Fig. 3(a)]. However, the molecular weight distribution results [Fig. 3(b)] show that even while conversion slows after ~ 3 h, the molecular weight (M_n) and PDI were observed to increase, from 9000 g/mol with a PDI of 5.9 after 3 h to 12,000 g/mol with a PDI of 10.3 after 4.5 h, reaching the gel point after 5 h. The precipitated hyperbranched polymer was found to be readily soluble in a number of solvents, including benzene, chloroform, dichloromethane, and PGMEA. A glass transition temperature (T_g) of 81 °C, lower than that for polystyrene (~ 104 °C) or poly(*t*-butyl methacrylate) (~ 118 °C)[38] was observed and it is instructive to compare these results with those obtained for hyperbranched polymers prepared by CTA and traditional free radical chemistry. In these cases, the highest reported crosslinker concentration was 12% and required 12% CTA, with a M_n and PDI of 5280 g/mol and 2.94 being obtained.[32]

In addition to structural changes during polymerization, GC and NMR results demonstrated changes in monomer incorporation with a decrease in the fraction of crosslinker in the hyperbranched polymer as the polymerization proceeds [Fig. 3(c)]. The initial polymer composition of 40 mol % crosslinker corresponds to the initial probability of incorporating crosslinker, which is defined by the fraction of vinyl groups that are contributed from the crosslinker (2 out of

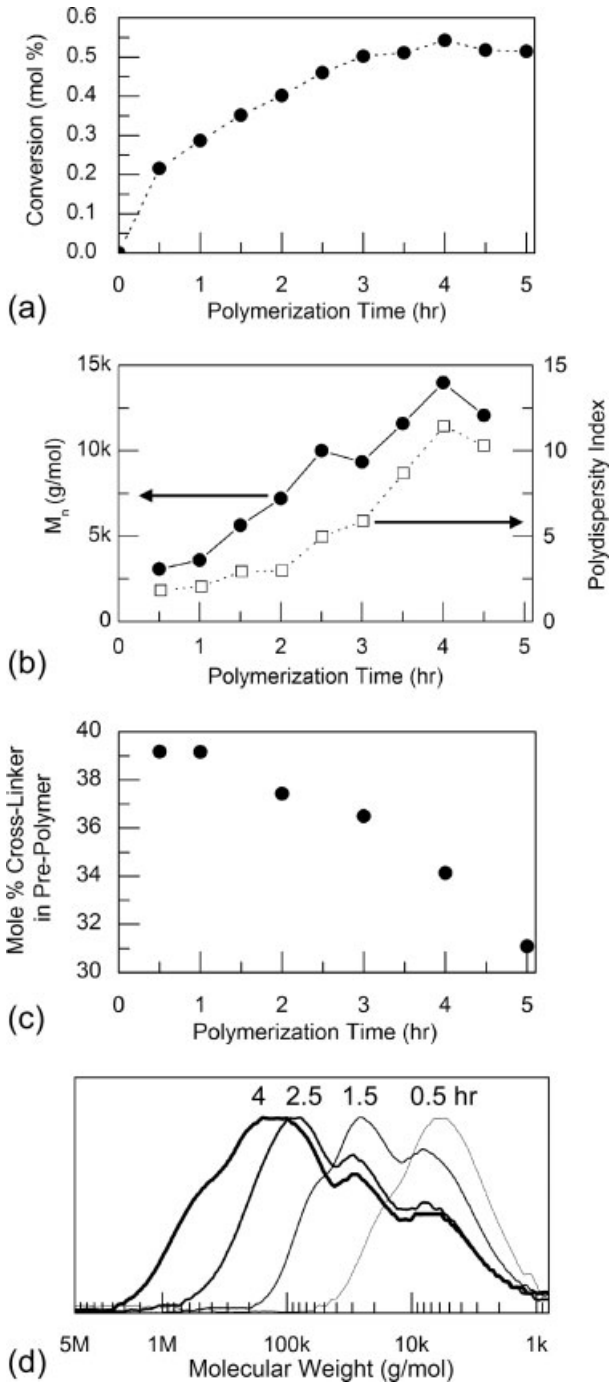

Figure 3. Variation of different parameters during the NMRP polymerization of a 3:1 molar ratio of styrene and 1,6-hexandediol dimethacrylate at 125 °C in toluene (25wt%): (a) conversion of monomer; (b) molecular weight (●) and polydispersity (□); (c) hyperbranched polymer mol % crosslinker; (d) polystyrene equivalent molecular weight distribution.

Table 1. Effect of Varying Monomer Concentration on Conversion, Molecular Weight, and Polydispersity for the Copolymerization of 3:1 Molar Ratio of Styrene and 1,6-Hexandediol Dimethacrylate in Toluene

Total Monomer Concentration	8% (wt %)	15% (wt %)	25% (wt %)
Conversion (%)	45	52	54
M_n (g/mol)	4,800	7,400	13,400
PDI	2.1	3.9	14.7

5, or 40%). Overtime, the amount of crosslinker incorporated into the hyperbranched polymer decreases, due to the decreased reactivity of the pendant vinyl groups for the mono-incorporated repeat unit when compared with unreacted crosslinker.[37,38] As the crosslinker is polymerized, the effective number of vinyl groups in the monomer mixture contributed from crosslinker also decreases and the changing composition of the hyperbranched polymer reflects changes in the composition of the monomer solution.

To optimize the polymerization conditions for both, low molecular weight and high conversions, the effects of monomer concentration and ratio of monofunctional monomer to crosslinker was studied. For NMRP polymerizations in particular, decreasing the monomer concentration has been shown to limit the molecular weight.[39] To take advantage of this effect, polymerizations were carried out in toluene with concentrations varying from 8 to 75 wt % monomer. For polymerizations at concentrations of 50 and 75%, the gel point was reached after 2 h. In contrast, lower concentration polymerizations were still soluble at 4.5 h, which allows the resultant hyperbranched polymers to be fully characterized (Table 1). Although the conversion decreased only slightly as the monomer concentration was reduced to 8%, the molecular weight was reduced by more than 50% and the PDI decreased by a factor of 7 when compared with the 25wt% material. This indicates that lower solution concentrations in the reaction mixture are beneficial in preparing lower molecular weight materials with a minimal loss in yield, a trend which agrees with results reported for traditional free radical polymer preparation.[31]

Although molecular weight distribution and chemical composition provide insight into the polymer structure, no information is provided on whether or not any pendant polymerizable (vinyl) groups are present. The presence of these groups and their secondary crosslinking is crucial to the successful imprinting of these materials. Therefore the hyperbranched polymer was purified by precipitation into methanol followed by centrifugation and ^{1}H NMR was used to determine the concentration of pendant vinyl groups (peaks at $\sim$ 5.5 and 6.1 ppm) present in the hyperbranched polymer (Fig. 4). For a sample polymerized for 2 h (M_n = 7200; PDI = 3.00), NMR studies showed that the molar crosslinker concentration is 42% and the molar concentration of singly reacted crosslinker is 12%, which is comparable to the values obtained by GC [Fig. 3(c)]. These values are significantly higher than those reported for free radical synthesis, which contained 2.6 to 11.0 mol % crosslinker and 0.6 to 3.8 mol % singly reacted crosslinker.[31,32] In these cases, singly reacted crosslinker is defined as a divinyl derivative that only undergoes reaction through one double bond while doubly reacted crosslinker refers to a molecule in which both double bonds have reacted. The higher incorporation of crosslinker and the increased level of pendant vinyl groups demonstrate the advantages of NMRP for the preparation of hyperbranched polymers, especially those targeted for UV-IL applications.

Functionalized Hyperbranched Polymer Synthesis

In defining the potential advantages of using hyperbranched polymers as resist materials,

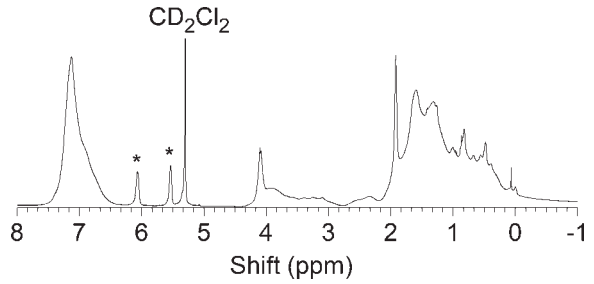

Figure 4. NMR spectra of hyperbranched polymer, **1**, formed from a 37.5:12.5:1 molar ratio of styrene: crosslinker:initiator. Stars show peaks representing pendant vinyl groups.

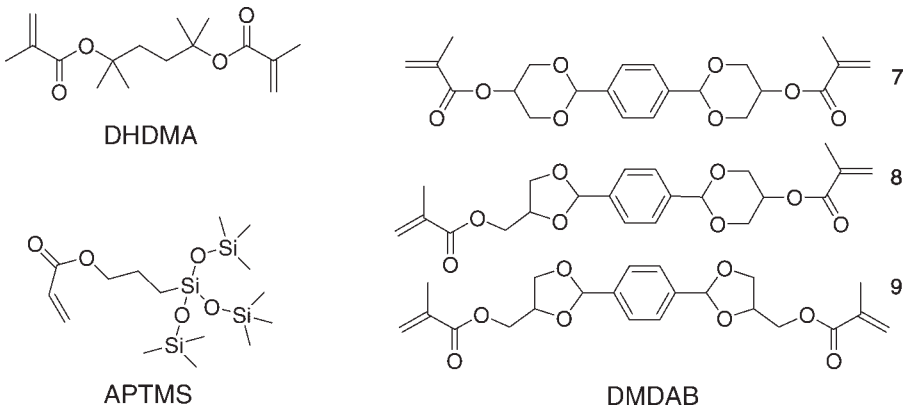

Figure 5. Representative structures of monofunctional and crosslinking monomers used in the synthesis of novel hyperbranched polymers for UV-imprint lithography.

three examples of monomers that could not be used in normal imprinting situations were examined. These include low boiling point monomers that evaporate during normal spin-coating, low solubility monomers that precipitate or crystallize during spin-coating and monomers that dewet during spin-coating. To demonstrate the applicability of hyperbranched polymers for the imprinting of each class of monomer, a total of four different polymers were prepared. The monomers used in these hyperbranched polymers include: MMA as an example of a low boiling point monomer; all structural isomers of DMDAB (Fig. 5), which are highly crystalline and have low solubility; APTMS (Fig. 5), which is a commonly used monomer to increase etch resistance to oxygen plasma etches[40] but suffers from severe dewetting during spin-coating; and 2,5-dimethyl-2,5-hexanediol dimethacrylate (DHDMA) (Fig. 5), which is an acid cleavable crosslinker that demonstrates retention of functionality after hyperbranched polymer formation. These monomers were then paired as needed during polymerization with either 1,6-hexanediol dimethacrylate or *p*-acetoxy styrene to form the desired hyperbranched macromolecule.

In each case, the polymerization conditions were based on the optimized results for the styrene and 1,6-hexanediol dimethacrylate system, 8 wt % total monomer concentration in toluene, 50:1 molar ratio of monomers to initiator, and a polymerization time of 2 h. For the DMDAB crosslinker which was not soluble in toluene, substitution of dioxane for toluene resulted in gel formation, so a 1:1 mixture of dioxane and toluene was used. Purification of the polymers consisted of evaporation of the solvent and any unreacted volatile monomer followed by precipitation.

After the appropriate work-up procedures were performed, the hyperbranched polymers were characterized by GPC (Fig. 6). Although polymerization conditions were identical in all but one case, hyperbranched polymers with a range of molecular weights/polydispersities and levels of repeat unit incorporation were obtained for the different monomer structures (Table 2). The polymer with the highest molecular weight was the copolymer of APTMS and 1,6-hexanediol dimethacrylate, whereas the lowest was the copolymer of *p*-acetoxy styrene and DHDMA (Fig. 6). This trend correlates with the variation in rate of radical polymerization of the different monomers families.[41]

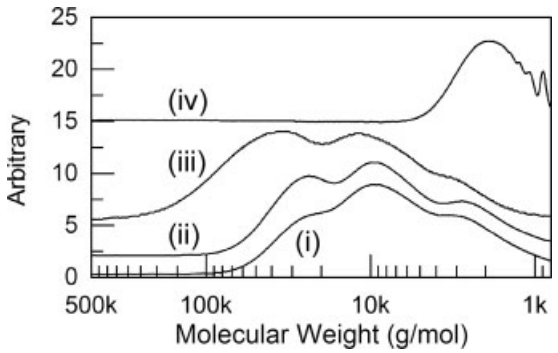

Figure 6. Molecular weight distribution for the purified hyperbranched polymers prepared from: (i) low boiling point monomer, MMA (M_n = 7300, PDI = 2.4); (ii) low solubility monomers, DMDAB (M_n = 9000, PDI = 2.3); (iii) dewetting monomer, APTMS (M_n = 14,900, PDI = 2.9); and (iv) functional crosslinker, DHDMA (M_n = 1800, PDI = 1.2).

Table 2. Composition (Mol % of Repeat Units) and Glass Transition Temperatures of Various Hyperbranched Polymers After Precipitation

Monomer System	MMA/ 1,6-hexanediol dimethacrylate	APTMS/ 1,6-hexanediol dimethacrylate	*p*-Acetoxy styrene/ DHDMA	Styrene/ 1,6-hexanediol dimethacrylate
Mol % of monomer in feed	40	59	74	58
Singly polymerized cross-linker	8	5	6	12
Doubly polymerized cross-linker	52	36	20	30
T_g (°C)	64	137	89	81

Thermal and Acid-Catalyzed Decomposition of DMDAB/DHDMA Crosslinkers

The decomposition of the DMDAB crosslinkers was examined by crosslinking a mixture of the isomers and then examining the weight loss both alone and in the presence of acid using TGA (Fig. 7). For comparison, the decomposition of crosslinked DHDMA is shown, with a weight loss at 225 °C indicating the decomposition of the tertiary ester group. The crosslinked DMDAB undergoes initial decomposition at 280 °C, representing deprotection of the acetals and evaporation of terephthalaldehyde, and a second weight loss at 370 °C. Although the weight loss due to decomposition of the acetal does not have a defined end, it occurs within the expected temperature range[40] and indicates a loss of $\sim$ 25%, which correlates with the expected 24% weight loss upon loss of the terephthalaldehyde. The other decomposition product, the methacrylate diol which is generated from singly polymerized crosslinker, must evaporate or decompose at the higher temperatures. Although the DMDAB crosslinker is stable to temperatures $\sim$ 60 °C higher than the DHDMA crosslinker, when the crosslinked DMDAB is heated in the presence of acid the decomposition temperature is lowered to 80 °C. This dramatic difference in decomposition temperature for a material with and without the addition of acid is characteristic of photoresists, and is a feature that was targeted in the design of the DMDAB crosslinker.

Comparison of Etch Resistance of Organic and Silicon-Containing Imprinted Films

One of the most interesting capabilities of UV-IL is the ability to incorporate a variety of different chemistries and reactive functional groups into the imprinted film. This allows the performance and properties of the imprinted features to be tailored to the desired application. This capability was demonstrated for hyperbranched macromolecules based on vinyl monomers by the incorporation of acid-labile linkages into the crosslinker and by the incorporation of repeat units having significant etch resistance. In the latter case, APTMS has been widely used as a repeat unit in etch barriers for organic substrates due to the high weight percentage of silicon in the repeat unit. Unfortunately as a monomer, APTMS undergoes severe dewetting during spin-coating and can therefore not be used in imprint formulations at the levels necessary to give etch resistance.[42]

To demonstrate the increased resistance to an oxygen plasma etch that can be achieved by the incorporation of a silicon-containing monomer, the etch rate of an APTMS hyperbranched polymer (61 mol % 1,6-hexanediol dimethacrylate, 39 mol % APTMS), containing 14 wt % silicon was compared to that of a DHDMA hyperbranched polymer (30 mol % DHDMA, 70 mol % *p*-acetoxy

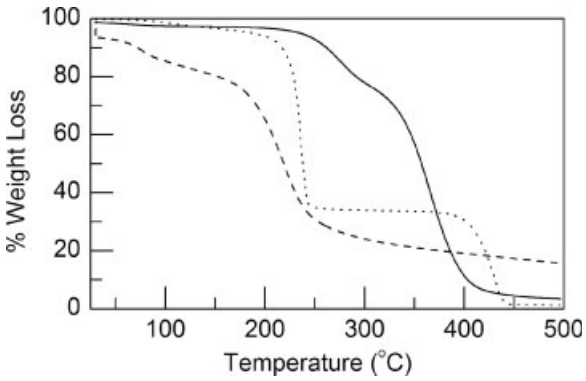

Figure 7. Thermal decomposition of crosslinked DMDAB with (dashed) and without acid (solid), compared to the decomposition of crosslinked DHDMA without acid (dotted).

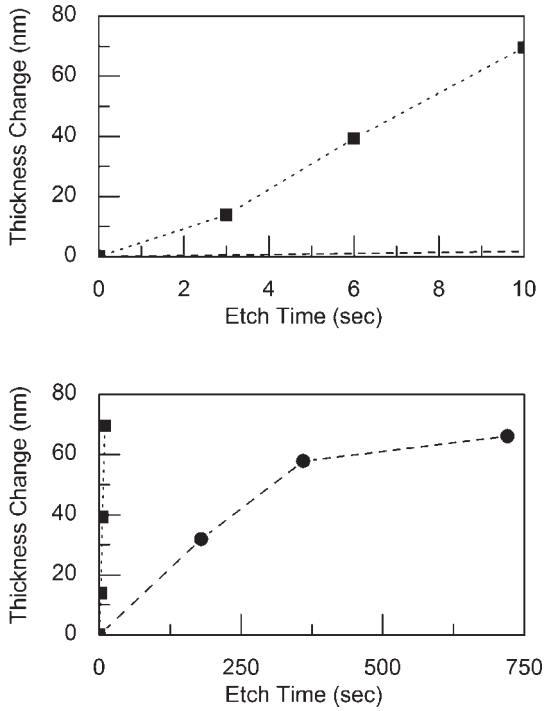

Figure 8. Etch resistance of (■) 30 mol % DHDMA, 70 mol % *p*-acetoxy styrene and (●) 61 mol % 1,6-hexanediol dimethacrylate, 39 mol % APTMS imprinted hyperbranched films.

styrene) (Fig. 8). Although the DHDMA hyperbranched polymer was etched quickly, at a rate of 7 nm/s, the silicon-containing hyperbranched polymer film was etched at a rate of only 0.2 nm/s. Additionally, after 360 s the etch rate of the silicon-containing film appears to slow even further, suggesting the formation of a silicon oxide film.

Stamping of Functionalized Hyperbranched Polymers

To demonstrate the application of hyperbranched polymers as a strategy for controlling the chemical composition of imprinted films, the four hyperbranched polymers were patterned with UV-IL (Fig. 1). When compared with a traditional small molecule UV-IL resist system, these hyperbranched polymers require different processing conditions such as longer exposure times to crosslink the films, though this can be decreased by diluting the hyperbranched polymer with a high boiling point monofunctional or crosslinking monomer. Visually the effect of hyperbranched polymer versus monomer mixture is dramatically demonstrated when the dewetting monomer (APTMS) system is compared. For the hyperbranched materials, uniform films were obtained, which displayed none of the characteristic dewetting that occurred for a film prepared from the monomers under identical concentrations on the same substrates (Fig. 9).

The robustness of using prepolymers as imprint resists was further demonstrated by achieving high resolution features for all four hyperbranched polymers even though the materials had a range of molecular weights, viscosities and level of vinyl group incorporation. The polymers were imprinted with stamps that contained a variety of feature shapes and sizes, and the patterned films were characterized with optical microscopy, SEM, and AFM. A representative sample of the images obtained with all four polymers is shown in Figure 10 and demonstrate the ability to pattern small and large features simultaneously. In addition, the patterning of both large open areas as well as large raised areas, which requires the flow of significant amounts of material, demonstrate the low viscosity and good flow characteristics of the hyperbranched materials.

Lithographic Patterning of Imprinted Hyperbranched Polymer Films

In addition to patterning with imprint lithography, two of the hyperbranched polymers were designed to allow for secondary patterning with photolithography.[43] Both the DHDMA and DMDAB crosslinkers contain acid-cleavable linkages, which allows for the crosslinked films formed from these materials to be selectively decomposed in the presence of acid. Such a capability allows these materials to be used in systems

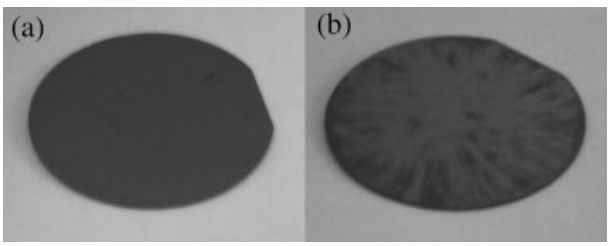

Figure 9. Silicon wafers coated with a self-assembled monolayer of 3-methacryloxypropyl trimethoxysilane and spin-coated with (a) hyperbranched polymer formed from APTMS and 1,6-hexanediol dimethacrylate and (b) APTMS and 1,6-hexanediol dimethacrylate monomers under identical concentrations (40 mol % APTMS, 60 mol % 1,6-hexanediol dimethacrylate, 7 wt % total monomer in PGMEA).

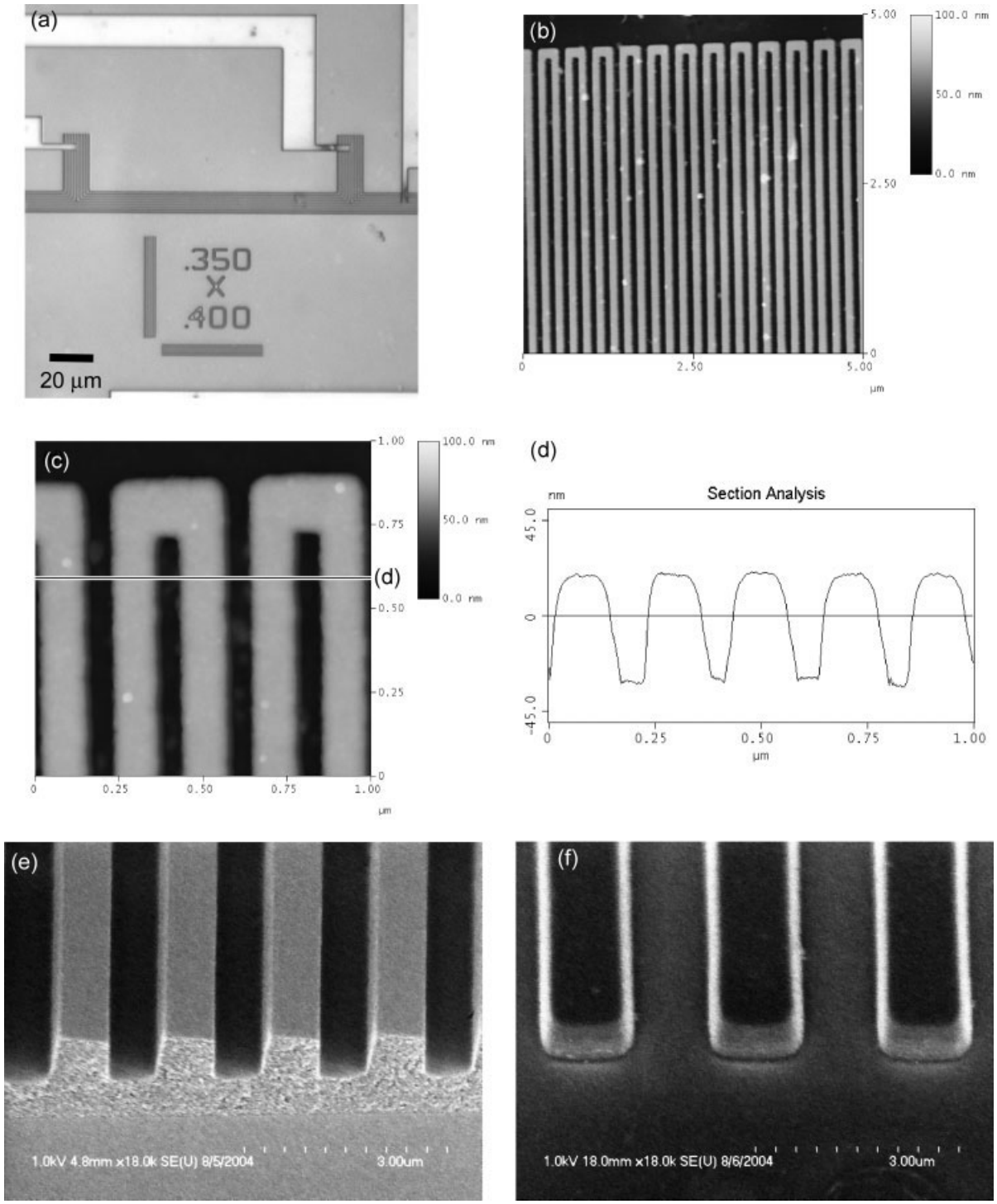

Figure 10. Characterization of patterned imprinted films. Optical microscope images: (a) APTMS polymer. AFM images (120 nm line width, 50 nm height): (b) DHDMA polymer; (c) APTMS polymer and (d) corresponding section analysis of image (c). SEM images: (e) methyl methacrylate polymer (cross-sectional image, 0.4 μm line width); (f) DMDAB polymer (30° image, 1.2-μm line width).

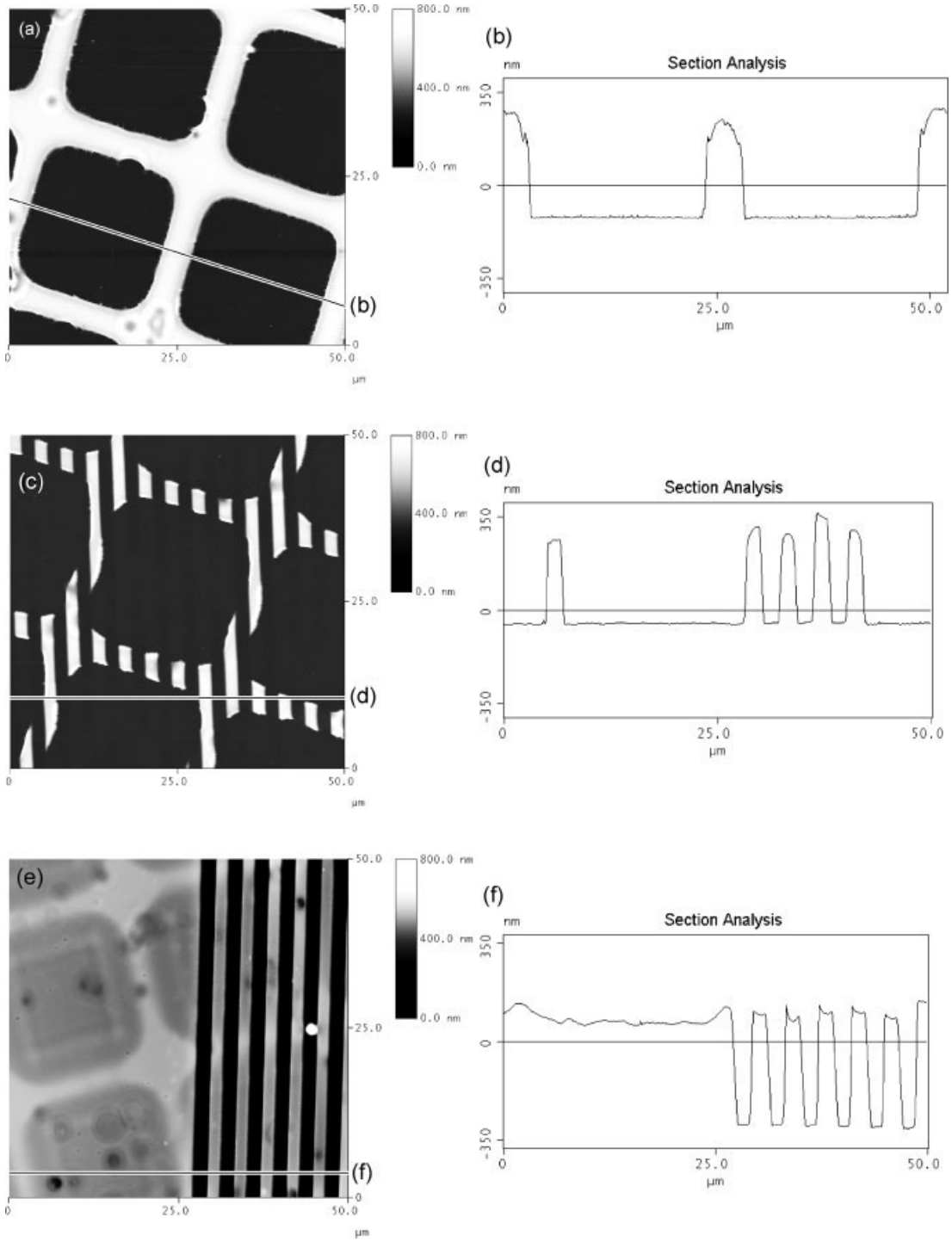

Figure 11. AFM images and corresponding section analyses of lithographically patterned films of: (a) and (b) flat crosslinked DHDMA hyperbranched polymer (360 nm film thickness, 4.5 μm lines); (c) and (d) imprinted crosslinked DHDMA hyperbranched polymer (330 nm film thickness, 2 μm width imprinted lines); (e) and (f) flat and imprinted crosslinked DMDAB hyperbranched polymer.

where it is necessary to remove the crosslinked films or for the creation of a wider range of features by combining imprint and optical lithography. The lithographic patterning of imprinted films formed from hyperbranched polymers also has the additional benefit of demonstrating that the polymer preparation and imprinting processes do not affect the structure of functional crosslinkers or involve unwanted side reactions leading to irreversible crosslinking.

The lithographic patterning procedure used for both imprinted and flat films formed from the DHDMA hyperbranched polymer involves exposure through a transmission electron microscope grid as a mask, followed by a bake time of 1 min at 110 °C. The resulting AFM image for the flat film shows the lithographically created grid-pattern with a height of 360 nm and a line-width of 4.5 μm [Fig. 11(a)]. The same grid-patterns appear in the image of the imprinted film; however, it is overlaid on top of lines which are 330-nm high and 2.0-μm wide [Fig. 11(b)]. These images demonstrate that the acid-cleavable functionality has been retained throughout the hyperbranched polymer preparation and imprinting.

Crosslinked films formed from the DMDAB hyperbranched polymer were also processed as described earlier, with a 200 mJ/cm^2 exposure dose. However, as shown in Figure 11, AFM indicates that only a 70 nm height change occurred from the photolithography. Although this is at first surprising, as the acetal protecting group has been used successfully in similar applications in photoresists,[44] the difference in the two systems lies in the fact that the acetal linkage requires catalytic amounts of water to undergo deprotection. In photoresist systems, this small amount of water can diffuse from the air into the film, allowing for deprotection of the acetal groups. In contrast, the imprinted films are coated with a thick layer of polystyrene and PAG, preventing the water from diffusing into the crosslinked film. While a small degree of deprotection occurs and results in a slight thickness change, to fully pattern the DMDAB crosslinked films either a different method for delivering the PAG or a technique for incorporating a small amount of water to the system would be necessary.

CONCLUSIONS

Hyperbranched polymers have been prepared from a variety of monofunctional and difunctional vinyl monomers and their use as resist materials imprint lithography examined. The molecular weight, PDI, and structural characteristics of the polymers could be controlled by varying the monomer structure and polymerization conditions, including concentration of monomer in toluene, ratio of monomer to initiator, and polymerization time. Polymers were prepared with concentrations of pendant polymerizable groups as high as 12 mol %, which is crucial to the application of these materials in UV-IL. The use of hyperbranched polymers in UV-IL allows for incorporation into the imprinted films of monomers which would otherwise be difficult to exploit using tradition monomer mixtures and standard conditions. To demonstrate this versatility, monomers which evaporate during spin-coating, that have low solubility in solvents used for spin-coating, and monomers which dewet during spin-coating were all successfully imprinted over large areas at high resolutions, with features as small as 120 nm. In addition, films were imprinted from hyperbranched polymer prepared with acid-cleavable crosslinkers (DHDMA), and these could then be patterned using photolithographic techniques. The preparation of hyperbranched polymers as resist materials for UV-IL is a simple and facile technique, which can greatly expand the range of chemistries and monomer systems that can be used with UV-imprint lithography.

The authors thank K. Carter and E. Hagberg for the use of the imprint lithography system and helpful discussions, R. Allen for use of the lithographic equipment, L. Li for thermal analysis, T. Magbitang for GPC measurements, B. Davis for SEM imaging, and M. Hart for oxygen plasma etching. This work was supported by the Semiconductor Research Corporation through the Graduate Fellowship Program, the Swedish Research Council (VR) Grant 2006-3617 and the National Science Foundation through the MRSEC program (DMR05-20415 for the UCSB MRL and the Center for Polymeric Interfaces and Macromolecular Assemblies).

REFERENCES AND NOTES

1. Xia, Y.; Rogers, J. A.; Paul, K. E.; Whitesides, G. M. Chem Rev 1999, 99, 1823–1848.
2. Gates, B. D.; Xu, Q.; Love, J. C.; Wolfe, D. B.; Whitesides, G. M. Annu Rev Mater Res 2004, 34, 339–372.
3. Gates, B. D.; Xu, Q.; Stewart, M.; Ryan, D.; Willson, C. G.; Whitesides, G. M. Chem Rev 2005, 105, 1171–1196.

4. International Technology Roadmap for Semiconductors, Semiconductor Industry Association, 2003. Available at http://public.itrs.net.
5. Kim, E.; Xia, Y.; Zhao, X.-M.; Whitesides, G. M. Adv Mater 1997, 9, 651–654.
6. Khang, D.-Y.; Lee, H. H. Appl Phys Lett 2000, 76, 870–872.
7. Chou, S. Y.; Krauss, P. R.; Renstrom, P. J. Appl Phys Lett 1995, 67, 3114–3116.
8. Chou, S. Y.; Krauss, P. R.; Renstrom, P. J. Science 1996, 272, 85–87.
9. Haisma, J.; Verheijen, M.; van den Heuvel, K.; van den Berg, J. J Vac Sci Technol B 1996, 14, 4124–4128.
10. Otto, M.; Bender, M.; Hadam, B.; Spangenberg, B.; Kurz, H. Microelectron Eng 2001, 57/58, 361–366.
11. Bender, M.; Fuchs, A.; Plachetka, H.; Kurz, H. Microelectron Eng 2006, 83, 827–830.
12. McClelland, G. M.; Hart, M. W.; Rettner, C. T.; Best, M. E.; Carter, K. R.; Terris, B. D. Appl Phys Lett 2002, 81, 1483–1485.
13. Kim, E. K.; Stacey, N. A.; Smith, B. J.; Dickey, M. D.; Johnson, S. C.; Trinque, B. C.; Willson, C. G. J Vac Sci Technol B 2004, 22, 131–135.
14. Bailey, T.; Choi, B. J.; Colburn, M.; Meissl, M.; Shaya, S.; Ekerdt, J. G.; Sreenivasan, S. V.; Willson, C. G. J Vac Sci Technol B 2000, 18, 3572–3577.
15. Komuro, M.; Tokano, Y.; Taniguchi, J.; Kawasaki, T.; Miyamoto, I.; Hiroshima, H. Jpn J Appl Phys Part 1 2002, 41, 4182–4185.
16. Taniguchi, J.; Kawasaki, T.; Tokano, Y.; Kogo, Y.; Miyamoto, I.; Komuro, M.; Hiroshima, H.; Sakai, N.; Tada, K. Jpn J Appl Phys Part 1 2002, 41, 4194–4197.
17. White, D. L.; Wood, O. R. J Vac Sci Technol B 2000, 18, 3552–3556.
18. Palmieri, F.; Adams, J.; Long, B.; Heath, W.; Tsiartas, P.; Willson, G. C. ACSNano 2007, 1, 307–312.
19. Hiroshima, H.; Komuro, M.; Kasahara, N.; Kurashima, Y.; Taniguchi, J. Jpn J Appl Phys Part 1 2003, 42, 3849–3853.
20. von Werne, T. A.; Germack, D. S.; Hagberg, E. C.; Sheares, V. V.; Hawker, C. J.; Carter, K. R. J Am Chem Soc 2003, 125, 3831–3838.
21. Montague, M.; Hawker, C. J. Mater Chem 2007, 19, 526–534.
22. Beinhoff, M.; Appapillai, A. T.; Underwood, L. D.; Frommer, J. E.; Carter, K. R. Langmuir 2006, 22, 2411–2414.
23. Ratner, B. D. J. Mol Recognit 1996, 9, 617–625.
24. Hench, L. L.; Polak, J. M. Science 2002, 295, 1014–1017.
25. Beebe, D. J.; Mensing, G. A.; Walker, G. M. Annu Rev Biomed Eng 2002, 4, 261–286.
26. Kricka, L. J. Clin Chem 1998, 44, 2008–2014.
27. Lebib, A.; Chen, Y.; Cambril, E.; Youinou, P.; Studer, V.; Natali, M.; Pepin, A.; Janssen, H. M.; Sijbesma, R. P. Microelectron Eng 2002, 61/62, 371–377.
28. Hao, J.; Lin, W. M.; Palmieri, F.; Nishimura, Y.; Chao, L. H.; Stewart, D. M.; Collins, A.; Jen, K.; Willson, G. C. Proc SPIE 2007, 6517, 6517291–6517299.
29. (a) Tsai, L. R.; Chen, Y. J Polym Sci Part A: Polym Chem 2007, 45, 5541–5551; (b) Scholl, M.; Nguyen, T. Q.; Bruchmann, B.; Klok, H. A. J Polym Sci Part A: Polym Chem 2007, 45, 5494–5508; (c) Krämer, M.; Kopaczynska, M.; Krause, S.; Haag, R. J Polym Sci Part A: Polym Chem 2007, 45, 2287–2303; (d) Li, J.; Sun, M.; Bo, Z. J Polym Sci Part A: Polym Chem 2007, 45, 1084–1092; (e) Murali, M.; Samui, A. B. J Polym Sci Part A: Polym Chem 2006, 44, 3986–3994; (f) Hawker, C. J.; Lee, R.; Fréchet, J M. J. J Am Chem Soc, 1991, 113, 4583.
30. (a) Powell, K. T.; Cheng, C.; Wooley, K. L.; Singh, A.; Urban, M. W. J Polym Sci Part A: Polym Chem 2006, 44, 4782–4794; (b) Lin, Y.; Liu, X.; Li, X.; Zhan, J.; Li, Y. J Polym Sci Part A: Polym Chem 2007, 45, 26–40; (c) Hawker, C. J.; Fréchet, J. M. J.; Grubbs, R. B.; Dao, J. J Am Chem Soc, 1995, 117, 10763–10764.
31. (a) O'Brien, N.; McKee, A.; Sherrington, D. C.; Slark, A. T.; Titterton, A.; Polymer 2000, 41, 6027–6031; (b) Slark, A. T.; Sherrington, D. C.; Titterton, A.; Martin, I. K. J Mater Chem 2003, 13, 2711–2720.
32. (a) Isaure, F.; Cormack, P. A. G.; Sherrington, D. C. J Mater Chem 2003, 13, 2701–2710; (b) Isaure, F.; Cormack, P. A. G.; Sherrington, D. C. Macromolecules 2004, 37, 2096–2105; (c) Sato, T.; Ono, A.; Hirano, T.; Seno, M. J Polym Sci Part A: Polym Chem 2006, 44, 2328–2337.
33. Ide, N.; Fukuda, T. Macromolecules 1997, 30, 4268–4271.
34. Ide, N.; Fukuda, T. Macromolecules 1999, 32, 95–99.
35. Kilian, L.; Wang, Z.-H.; Long, T. E. J Polym Sci Part A: Polym Chem 2003, 41, 3083–3093.
36. Benoit, D.; Chaplinski, V.; Braslau, R.; Hawker, C. J. J Am Chem Soc 1999, 121, 3904–3920.
37. Okay, O.; Kurz, M.; Lutz, K.; Funke, W. Macromolecules 1995, 28, 2728–2737.
38. Polymer Handbook, 4th ed.; Brandrup, J.; Immergut, E. H.; Grulke, E. A., Eds. Wiley: New York, 1999.
39. Hawker, C. J.; Barclay, G. G.; Orellana, A.; Dao, J.; Devonport, W. Macromolecules 1996, 29, 5245–5254.
40. Colburn, M.; Grot, A.; Choi, B. J.; Amistoso, M.; Bailey, T.; Sreenivasan, S. V.; Ekerdt, J. G.; Willson, C. G. J Vac Sci Technol B 2001, 19, 2162–2172.

41. Odian, G. Principles of Polymerization, 3rd ed.; Wiley: New York, 1991.
42. Goken, H.; Esho, S.; Ohnishi, Y. J. Electrochem Soc 1983, 130, 143–146.
43. (a) Moreau, W. M. Semiconductor Lithography; Plenum: New York, 1988; (b) Macdonald, A. S.; Wilson, C. G.; Fréchet, J. M. J. Acc Chem Res 1994, 27, 151–158; (c) Itoh, H.; Wilson, C. G. Polym Eng Sci 1983, 23, 1012; (d) Ito, H.; Wilson, C. G.; Fréchet, J. M. J. U.S. Patent 4,491,628, 1985; (e) Jhaveri, S. B.; Beinhoff, M.; Hawker, C. J.; Carter, K. R.; Sogah, D. Y. ACS NANO, 2008, 2, 719–727; (f) Heath, W. H.; Palmieri, F.; Adams, J. R.; Long, B. K.; Chute, J.; Holcombe, T. W.; Zieren, S.; Truitt, M. J.; White, J. L.; Willson, C. G. Macromolecules 2008, 41, 719–726; (g) Ogura, T.; Ueda, M. J Polym Sci Part A: Polym Chem 2007, 45, 661–668.
44. Jiang, Y.; Bassett, D. R. In Polymers for Microelectronics; Thompson, L. F.; Willson, C. G.; Tagawa, S., Eds.; American Chemical Society: Washington, DC, 1994; Vol. 537, pp 40–52.